MS-No.: os-2020-33

Version: Revision

Title: Subsurface Initiation of Deep Convection near Maud Rise

Author(s): René M. van Westen and Henk A. Dijkstra

Point-by-point reply to reviewer #1

September 24, 2020

We thank the reviewer for his/her careful reading and for the useful comments on the manuscript. Below is a point-by-point reply with references to figures which are placed at the bottom of the document.

Major comments:

1. *(...) They also do not investigate several previously suggested significant preconditioning processes that are relevant to the Maud Rise and the Weddell Sea, including the size of the sub-surface heat reservoir created by accumulation of Warm Deep Water, the strength of the Taylor column associated with the Maud Rise seamount, the strength of the impinging flow, and surface salinity anomalies. (...)*

   Author's reply:
   The reviewer is correct that additional preconditioning processes can play a role near Maud Rise. In the revision of van Westen and Dijkstra (2020, https://doi.org/10.5194/os-2020-25, in review) we included an analysis of the surface salinity anomalies, SAM index, and Taylor columns. There is no link between the multidecadal preconditioning near Maud Rise and the SAM index in the CESM. There are indeed Taylor columns present near Maud Rise which precondition the region. These Taylor columns are present over the entire simulation period, but cannot explain the multidecadal time scale of polynya formation.

   In the revision here, we have focussed more on the salinity anomalies in the mixed layer prior to Maud Rise Polynya (MRP) formation. We find that the surface is slightly saltier prior to MRP formation with a magnitude of 0.07 Psu w.r.t. the time mean (Figure 1c). Part of these anomalies are related to enhanced Ekman upwelling which entrains salt

from below the mixed layer depth (Figure 1d). However, these salinity anomalies are too weak to induce convection near the surface.

Changes in manuscript:
In the revision we will mention all of the relevant preconditioning processes, referring also to results in van Westen and Dijkstra (2020). Note that the current manuscript mainly focusses on the initiation of convection near Maud Rise and not on the preconditioning, but we agree with the reviewer that this should be placed into context. The surface salinity analysis will be included in the revised results section.

2. *In section 3.1, the authors show the accumulation of subsurface heat and salt prior to the onset of the polynyas but fail to relate it to the heat and salt content of a warm and salty water mass known as the Weddell Deep Water (WDW) which lies between 250- 1500m in the Weddell Sea. A necessary but not sufficient condition for long-lasting, consecutive winter polynyas to occur is the heat reservoir at depth or the heat content of WDW (Martinson et al. 1981; Martin et al. 2013; Cheon et al. 2015; Dufour et al. 2017; Kurtakoti et al. 2018). If the main result in the paper is that the convection is initiated subsurface, a thorough and robust analysis of the stratification and water masses in and around Maud Rise is critical to the authors' justification and the readers' understanding.*

Author's reply:
We analysed the properties (e.g. temperature and salt) of the Weddell Deep Water (WDW) in more detail. The WDW properties and depth profiles reasonable match with that of observations, but the modelled WDW is slightly warmer and more saline compared to observations (Figure 2; note that the CESM simulation had a spin-up period of 150 years). Observed trends of the WDW are also represented in the CESM and there is no spurious build-up of heat as reported in several low-resolution models. The highest temperature and salinity values of the WDW are found prior to polynya formation. This is in agreement with the subsurface static instabilities which develop prior to MRP formation. During MRP formation, the temperature and salinity of the WDW decrease, also seen in observational records.

Changes in manuscript:
We will include an analysis of the properties (e.g. temperature and salt)

of the WDW and discuss the relevant trends of these properties. We will also include a comparison with observational results of the WDW.

3. *Please define what is subsurface convection. How is it triggered and how is it maintained? Is this convection that only occurs within the WDW and if so how is it initiated and how is this sustained?*

Author's reply:
There are three different types of oceanic convection (Akitoma 1999, Su et al. 2016): convection by buoyancy loss (type I convection), thermobaric convection (type II convection) and thermobaric cabbeling (type III convection). A nonlinear equation of state is essential only for the latter two types. In type I convection, the mixed layer gradually deepens by the loss of surface buoyancy. Near Maud Rise, surface buoyancy loss occurs at the surface when the surface is strongly cooled during Austral winter time and by the contribution of sea-ice formation (e.g. brine rejection). In the CESM, the mixed layer depth is seasonally varying prior to MRP formation (Figure 4). In most MRP literature, only the negative surface buoyancy (by positive salinity anomalies) is considered. Parcels with a negative buoyancy sink and mix with the layers below and reach their equilibrium buoyancy, this depth marks the mixed layer depth.

However, the build-up of a subsurface heat reservoir (Figure 2) induces buoyancy gain by thermal expansion. Parcels located at subsurface depths experience an upward force and mix with the layers above. These upward moving parcels also reach a certain equilibrium buoyancy (with some overshooting by inertia). The upward motion of parcels at subsurface depths is the definition of subsurface convection in the manuscript. The maximum vertical extent of the subsurface convection can be measured using the depth-integrated buoyancy:

$$B(z) = -\int_{-z_{ref}}^{-z} g\frac{\rho_\theta(-z_{ref}) - \rho_\theta(z')}{\rho_\theta(z')}\,\mathrm{d}z' \tag{1}$$

In the previous version of the manuscript, we confusingly referred to the expression above as CAPE. The large subsurface heat reservoir below Maud Rise maintains the subsurface convection and convection ceases when it is depleted.

Note that subsurface convection plays a dominant role in the initiation of MRP in the CESM during model year 231. Subsurface instabilities (Figure 3) vertically mix heat and salinity towards the surface. The following model year 232, the surface is relatively warm and saline and the surface becomes unstable by buoyancy loss (Figure 4b).

Changes in manuscript:
We will not use CAPE anymore in the revised manuscript and we will better specify the type of convection (i.e. buoyancy loss and gain).

4. *One of the major scientific weaknesses of this study is the context in which CAPE is used. Ocean CAPE is defined for an ocean column as the maximal Potential Energy that can be released by adiabatic vertical parcel rearrangements, arising from thermobaricity (Su et al. 2016a,b). However, that alone does not indicate the onset of deep convection. Fig 3a. is used to indicate the onset of subsurface convection in early-mid July which is not accurate. Fig 3c clearly shows that the subsurface pattern repeats it- self in the 2 years prior to the formation of the polynyas. This only indicated weakening subsurface stratification and not the onset of subsurface convection which is consistent with the accumulation of WDW heat content. If we could also see the Hovmöller of Temperature and Salinity time series that overlaps the time periods used in 3a and 3c, we can then confidently know for sure if convection does begin in the subsurface as claimed by the authors.*

Author's reply:
To determine precisely where the vertical mixing occurs near Maud Rise in the CESM, we have re-run model year 231 and written out the daily-averaged vertical diffusivities. Convection can be recognised in climate models by the occurrence of large values to the vertical diffusivity (Figure 3c). We find that the subsurface starts to mix and this mixing becomes stronger prior to MRP formation. In the surface layer, there is also some mixing, but the vertical diffusivity values are a factor 3 smaller compared to that of the subsurface prior to MRP formation (Figure 3d). Using the final depth of the parcels (red curve in Figures 3b,c, buoyancy), we find that below (above) this depth high (low) values of vertical diffusivity are found. This suggests that the maximum vertical extent of the region of large vertical diffusivity can be captured by using the definition of depth-integrated buoyancy. The

daily-averaged Hovmöller diagram of vertical diffusivity is similar to the static instability diagram (compare Figure 3a and 3c). There is a clear relationship between the magnitude of static instabilities and the vertical diffusivity (Figure 3d).

As mentioned by the reviewer, there are indeed subsurface static instabilities in model year 229 and 230 (Figure 4a). However, the magnitude of these static instabilities is much smaller compared to the ones in model year 231. For example, when taking the depth-averaged and monthly-averaged static instabilities between 200 – 1000 m depths (Figure 4b), the subsurface static instabilities are a factor 4.8 (August model year 229) and 7.9 (August model year 230) smaller compared to August model year 231. Smaller static instabilities result in less vertical diffusivity which do not overcome the stratification near the surface.

Changes in manuscript:
We will include the analysis of the daily-averaged vertical diffusivity in the manuscript. We will demonstrate that the subsurface static instabilities are much larger than the surface static instabilities. A link will made with the WDW and the surface salinity anomalies.

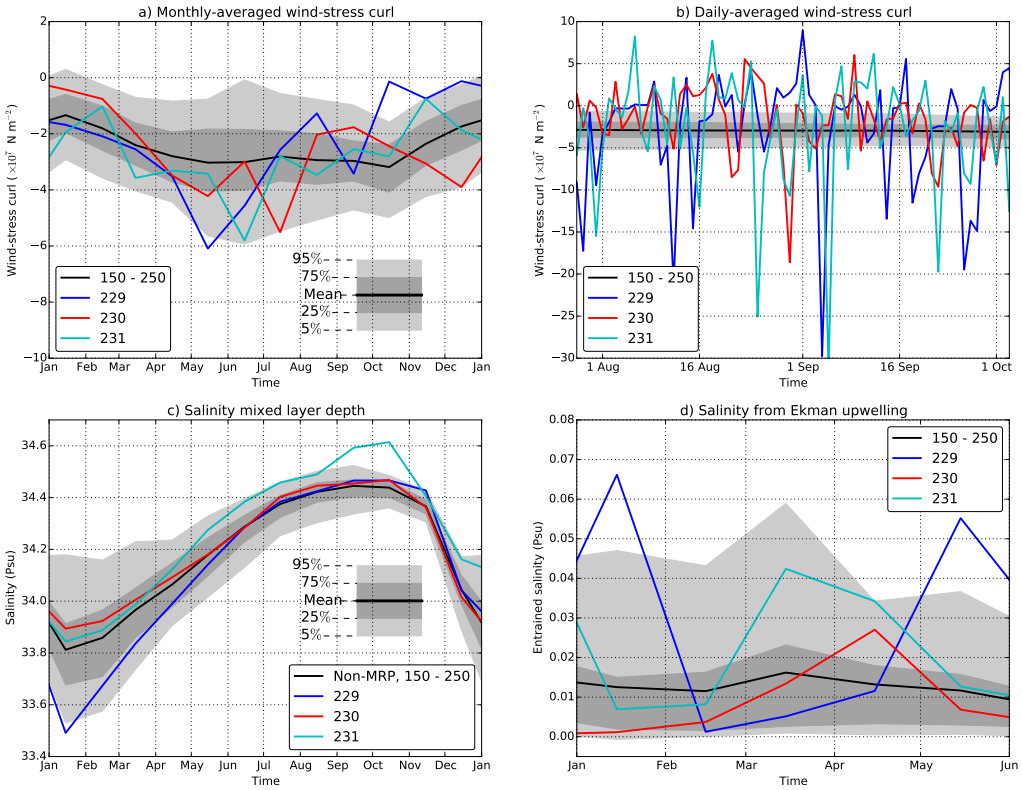

Figure 1: (a): Monthly-averaged magnitude of the wind-stress curl over the Polynya region for model years 229, 230 and 231. The shading indicates the climate variability, where the dark (light) shading correspond to the 25% – 75% (5% – 95%) percentile levels, the black curve is the climatology mean (model years 150 – 250). (b): Same as a), but now for daily averages. The shading is the same as in a). (c): Depth-averaged salinity over the mixed layer depth for model years 229, 230 and 231. The shading indicates the climate variability of this quantity (same as a)), but now only the non-MRP years are considered in the climatology. (d): The entrained salinity into the mixed layer from Ekman dynamics for model year 229, 230 and 231. The shading indicates the climate variability of this quantity (same as a)).

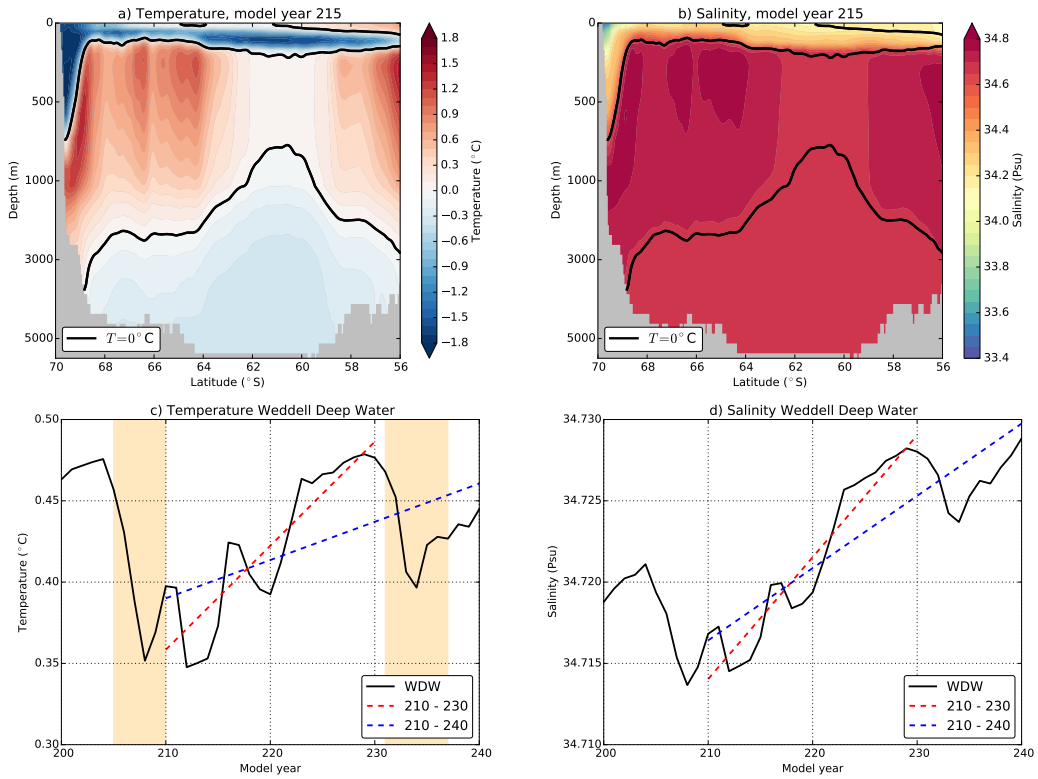

Figure 2: (a & b): Zonal mean (1°W – 1°E) of temperature and salinity along the Greenwich Meridian. The displayed values are yearly averages for model year 215. The black contour displays the 0°C, which marks the WDW. (c & d): Time evolution of the temperature and salinity of the WDW. The dashed lines are linear trends between model years 210 – 230 (red) and model years 210 – 240 (blue). The shading indicates the polynya years.

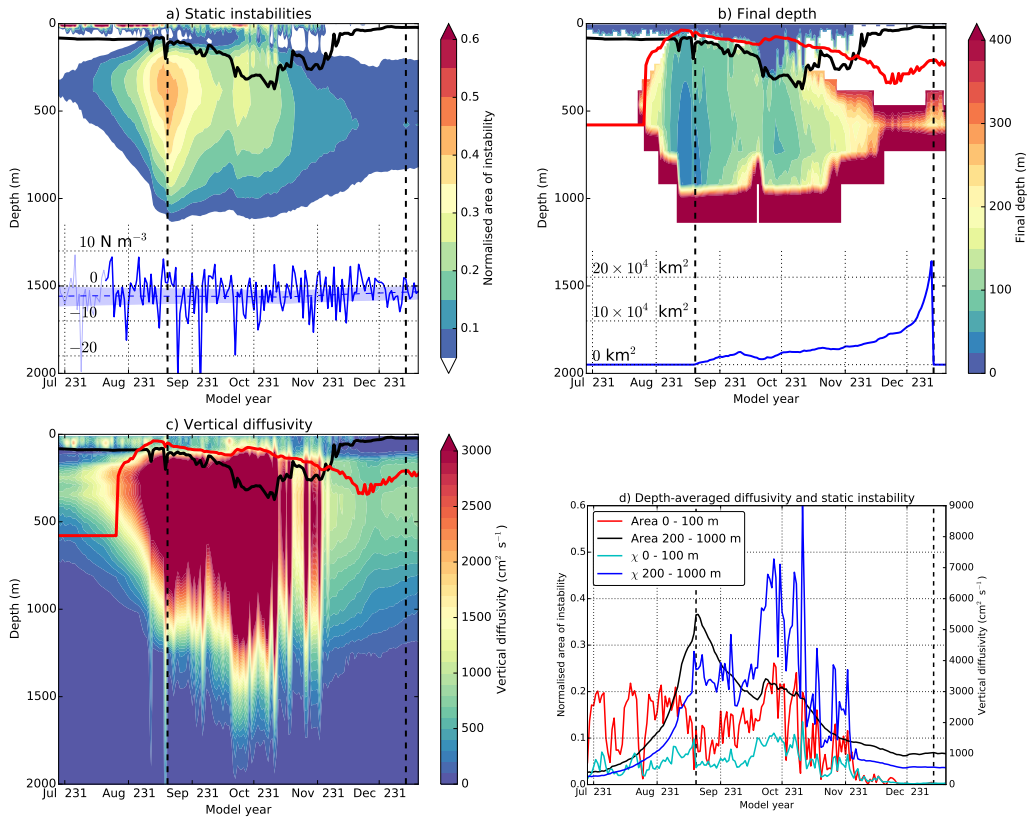

Figure 3: (a): Area per depth level where the water column in the Polynya region is statically unstable ($\mathcal{S} > 0$), normalised to the total area at that depth level. The blue curve is the daily-averaged magnitude of the wind-stress curl over the Polynya region, same as in Figure 1b. (b): Final depth of fluid elements due to (subsurface) convection. Only regions where deviations from the initial depth occur are displayed. The red curve shows the final depth of convection initially starting at $z_{ref} = 580$ m. The blue curve (bottom part) is the total area of the model year 231 MRP. (c): The vertical diffusivity (χ) for temperature, spatially averaged over the Polynya region. The red curve is the same as in b). In a) – c), the black curve shows the maximum mixed layer depth spatially averaged over the Polynya region. (d): The depth-averaged vertical diffusivity (χ) and normalised area of static instabilities over the upper 100 m and between 200 – 1000 m. In all figures, the dashed lines indicate the formation (20 August) and ending (14 December) of the MRP.

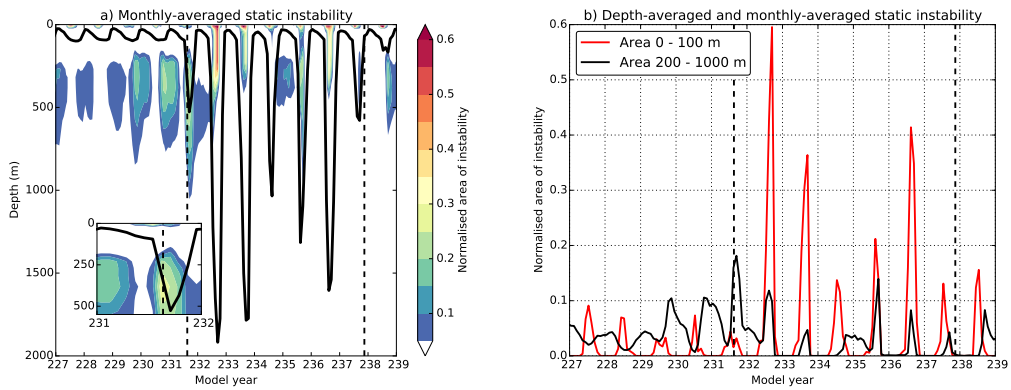

Figure 4: (a): Area per depth level where the water column in the Polynya region is statically unstable ($\mathcal{S} > 0$), normalised to the total area at that depth level. (b): The depth-averaged normalised area of static instabilities over the upper 100 m and between 200 – 1000 m. In both figures, the dashed lines indicate the beginning (model year 231) and ending (model year 237) of the multiyear MRPs. The model output analysed consists of monthly averages.